Slope instrumentation and unsaturated stability evaluation for steep natural slope close to railway line

H. Heyerdahl
Risk, slope stability and climate adaptation section, Natural Hazards division, Norwegian Geotechnical Institute (NGI); Department of Geosciences, Faculty of Mathematics and Natural Sciences, University of Oslo

Ø.A. Høydal & K. G. Gisnås
Avalanches and Rockslides section, Natural Hazards division, NGI, Norway

Y. Kvistedal
Geosurveys section, Natural Hazards division, NGI, Norway

P. Carotenuto
Laboratory and Model testing section, Offshore Energy division, NGI, Norway

ABSTRACT: The paper presents an instrumented natural soil slope in Eastern Norway. The slope is steep, 25-30 m high, and located adjacent to an existing railway track. Due to areas with protected cultural heritage behind the slope crest, options for physical slope stabilizing measures are limited. The ground conditions consist of 8-10 m sand and silt over marine clay to large depth. The steep upper part of the slope (inclination > 45˚) is theoretically unstable, unless considerable true or apparent cohesion is included. The effect of soil suction and infiltration in the vadose zone should therefore be evaluated. Stability calculations with unsaturated soil parameters were performed, based on retention curves for sand and silt and triaxial tests. The slope was instrumented with soil moisture sensors, temperature sensors and piezometers. Observed changes in the water contents and pore-water pressure were small and slow. Landslide risk was evaluated from in situ measurements and from "design rainfall" for the site. Conclusions drawn with respect to frequency of possible landslide events indicate return periods of more than 100 years.

1 INTRODUCTION

As part of an InterCity railway project in Eastern Norway, an additional railway track is being planned next to an existing railway line (Fig. 1). The upper part of the natural slope west of the existing track is very steep, with a slope angle of more than 45˚. A problem for the project is the area at the west of the slope, containing cultural heritage objects such as-church, old graveyard, etc. Physical slope stabilizing measures should be avoided within the marked area in Figure 1.

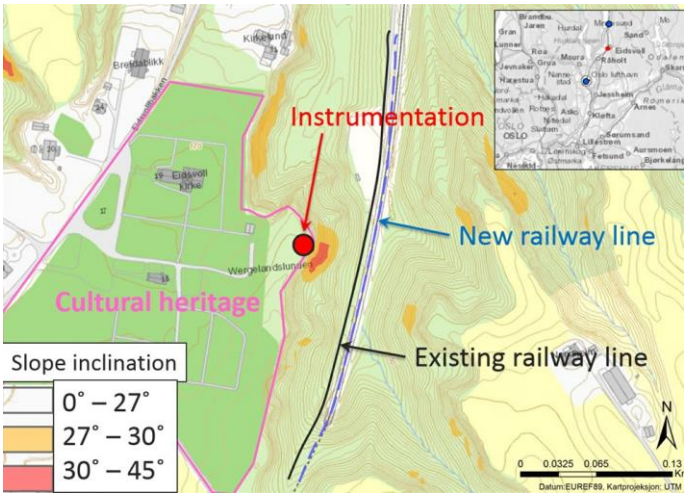

Figure 1. Study area with instrumented site at Eidsvoll, Eastern Norway.

2 GROUND CONDITIONS

A layer of approx. 10 m sand/silt lies on top of a thick layer of firm marine clay extending to large depth (Fig. 7). The slope is 25-30 m high, but only the upper part of the slope (the top layer of sand and silt) is the concern of this paper. Stability of deep-seated failure in clay is not discussed.

Grain size distribution analysis was performed for a number of representative (auger) samples from the sand/silt layer (Fig. 2). Cylinder sampling of undisturbed samples was difficult due to firm ground. Only one cylinder sample was successfully retrieved, and only partially filled with soil when extracted.

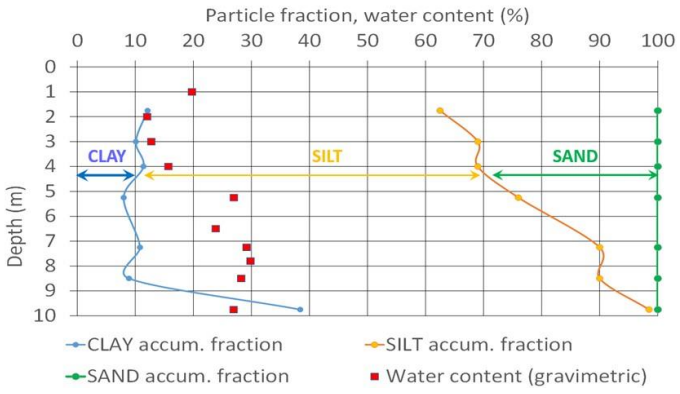

Figure 2. Grain size distribution of sand and silt layer.

The silt fraction increases with depth from approx. 50% at the plateau on top of the slope to approx. 80% at 9 m depth, while the sand fraction at the same time decreases from approx. 40% to 10%. The clay content is stable at approx. 10% down to 9 m; at this depth, the transition to the underlying clay layer is sharp, and at 10 m, the soil is characterized as clay (60% silt while sand vanishes completely). The gradual change in distribution between the three main grain size fractions creates some problems with characterizing the slope for modelling purposes.

Water content during sample opening was measured and showed increasing values with depth (Fig. 2). Gravimetric water contents close to 30% from 7 m depth indicate that the soil here is fully saturated.

3 RETENTION CURVES

Retention main drying curves were measured using a pressure plate apparatus at NGI's environmental laboratory. Based on visual inspection of all bag samples down to 10 m, samples were combined in batches of more or less equal soil. From these batches, soil was taken for retention tests. Specimens were compacted into test cups for the pressure plate apparatus (12 from each batch that was tested). After positioning the test cups on the filter plates (after weighing and sampling for measurement of water content), air pressure was applied stepwise in the pressure plate test chamber to apply suction by axis translation (Hilf 1956).

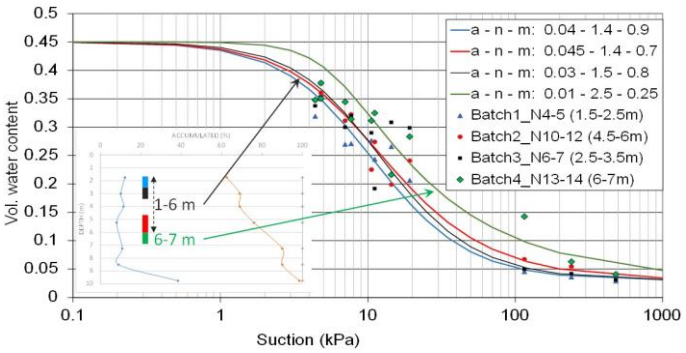

Figure 3. Retention main drying curves. Depth of batches indicated.

A curve-fitting equation (van Genuchten 1980) was used to produce continuous retention curves from the laboratory results. Based on the curves, it was concluded that Batch1, Batch2 and Batch3 between 1.5 and 6 m could be considered to have comparatively equal retention properties, while Batch4 at 6-7 m was different (larger water content at equal suction). The sand/silt layer was modelled as two main soil layers in the seepage analyses.

A few triaxial tests were performed. One saturated undrained test was performed on an intact specimen from 3.2 m depth, taken from the only sample cylinder that was successfully extracted from the firm soil. (This is a typical feature of silt, which may appear very firm during drilling or sampling, but loses all strength in contact with running water at exposed surfaces). The saturated test dilated heavily (Fig. 4), resulting in a large increase in shear strength due to the development of negative pore water pressure (suction) in the specimen during undrained shearing. To get some idea of the unsaturated shear strength, two active, drained, unsaturated (constant water content) shear tests were performed. In the intact specimen, saturated water content was w = 30.5%, corresponding to a void ratio e equal to 0.804. This void ratio was the target for enclosure of the compacted triaxial specimens.

The two unsaturated tests were initially planned with gravimetric water contents w of 20% and 25%, respectively. The specimen with planned water content of 25% was difficult to prepare, and water content had to be reduced to 21.5%. Based on the curves for shear stress versus axial strain (Fig. 4), the test at 20% water content seemed rather successful with a clear peak, while the behaviour of the test with 21.5% seems less reliable, with a very flat shear stress curve beyond the peak stress. Comparing values from the two compacted tests therefore offers problems, since the curves are very different. The peak of the test run at 20% water content is reached at vertical strain of approx. 4.5%, while the peak of the test at 21.5% is reached around 1% axial strain.

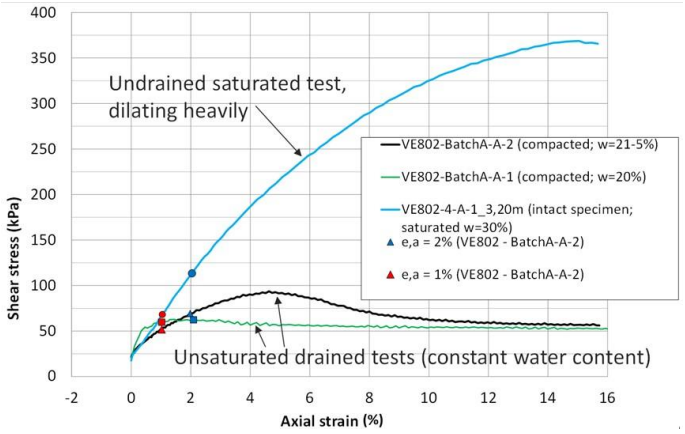

Figure 4. Active triaxial tests. One undrained, saturated test on intact specimen. Two drained, unsaturated tests on compacted specimens (constant water content).

Although suction in the compacted, unsaturated specimens is not known, it is possible to check whether there was in fact some effect of suction on the resulting shear strength. A rather conservative plot of the failure line for the two unsaturated, drained tests (whereof only one is trustworthy) confirms that there is a clear increase in (apparent) cohesion from saturated to unsaturated tests (Fig. 5). The tests were consolidated anisotropically, with consolidation stresses σ'_v = 60.8 kPa and σ'_h = 27.4 kPa (σ'_v was 66.4 kPa in the compacted test with water content w = 21.5%). The consolidation stress was

equivalent to calculated in situ stress at 3.2 m (the depth of the intact specimen).

The effective friction angle may be interpreted from the saturated undrained test to at least $\phi' = 35°$, or higher. Effective cohesion c' is however not easily determined from only one saturated, undrained test, and may be rather arbitrarily chosen. A cohesion value c' of 8-10 kPa may be appropriate (Fig. 5). For the intact cylinder specimen, saturated hydraulic permeability was measured at the end of the test to k = 2.4E-06 m/s. An effective friction angle of $\phi' = 36.9°$ was previously measured for a shallow silt sample from the same region (Heyerdahl and Pabst 2017), while saturated permeability was measured to approx. k = 1.0E-06 m/s (Heyerdahl 2017).

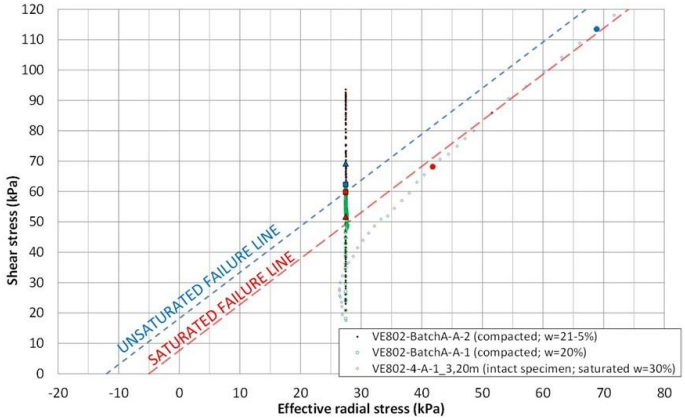

Figure 5. Interpretation of active triaxial tests. Saturated and unsaturated failure lines are proposed.

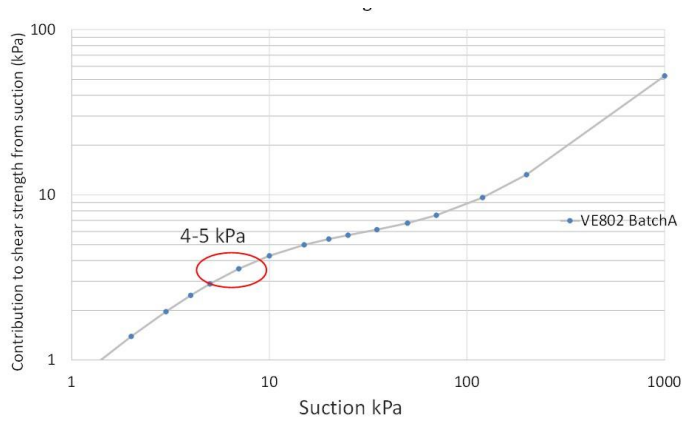

Figure 6. Estimate of unsaturated strength using Vanapalli 1st prediction method, combined with retention curve from Fig. 3.

Matric suction is principally unknown for the compacted triaxial specimens. Using the connection between suction and water content from the retention curve, the effect on shear strength of water content/suction may be estimated, e.g. by use of the Vanapalli's 1st method (Vanapalli et al. 1996) for prediction of unsaturated shear strength τ_{peak} (Eq. 1):

$$\tau_{peak} = c' + \tan\phi'(\sigma - u_a) + \Theta^{\kappa}(u_a - u_w)\tan\phi' \qquad (1)$$

where Θ is normalized water content; κ is an exponent; σ_v is total stress; u_a is air pressure; $(\sigma - u_a)$ is net stress; u_w is water pressure and $(u_a - u_w)$ is matric suction.

Application of Eq. 1 with the appropriate retention curve from Figure 3 gives an estimate for shear strength as function of suction (Fig. 6). For gravimetric water content w of approx. 20% in compacted specimens (corresponding to approx. 30% volumetric water content), Figure 3 shows that the equivalent suction is somewhat below 10 kPa.

4 IN SITU SLOPE INSTRUMENTATION

In order to investigate the hydrogeological conditions in the slope, in situ instrumentation of the slope was suggested, and accepted by the client. The motivation for in situ instrumentation was to monitor variation in soil moisture and pore-water pressure throughout the year, in order to compare these data with assumed infiltration from rainfall and snowmelt, as well as with the numerical model. Instruments were installed in late spring/ early summer of 2016. Figure 7 shows position of sensors in a cross section through the slope. In the top layer of sand/silt, combined soil moisture and ground temperature sensors were installed at 6 depths: 0.1 m, 0.5 m, 1 m, 2 m, 4 m and 6 m. In addition, piezometers were installed at depths 6 m, 9 m, 15 m and 23 m. For the two deepest piezometers the sensor is within the clay layer, while the two upper piezometers are in the silt layer. Holes for installation of sensors were prepared with a geotechnical drilling rig (Fig. 8).

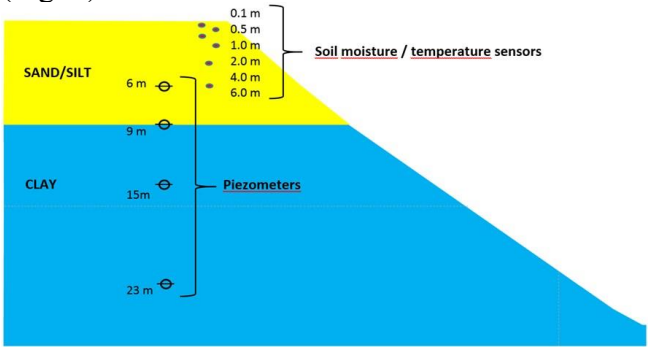

Figure 7. Cross section through the slope with position of in situ slope instrumentation. Combined soil moisture and temperature sensors down to 6 m, piezometers from 6 m to 23 m.

Figure 8. Installation of slope instrumentation close to the slope crest using a geotechnical drilling rig.

5 SLOPE INSTRUMENTATION RESULTS

Data for measured water contents from soil moisture sensors indicate that, soil moisture in the slope vary within narrow limits (Fig. 9). The five uppermost sensors all have volumetric water content lower than 25%. Saturated soil has a volumetric water content of 45-50%, implying that the soil is far from saturated. Exceptions are some "spikes" in the curve where the water content increases. Sensors at depths 0.1 m and 0.5 m follow each other when it comes to long-term variations, but short-term variations at 0.1 m are smoothened/smeared out at 0.5 m. Short-term changes at 0.1 m coincide with rain scours (Fig. 9). Water contents at 1-6 m depth change slowly throughout the period, and in situ water contents vary within a few percent. A small decrease in water content was logged for all sensors from 1 m and below. This period in fact was quite dry (verified by rainfall data in Fig. 9).

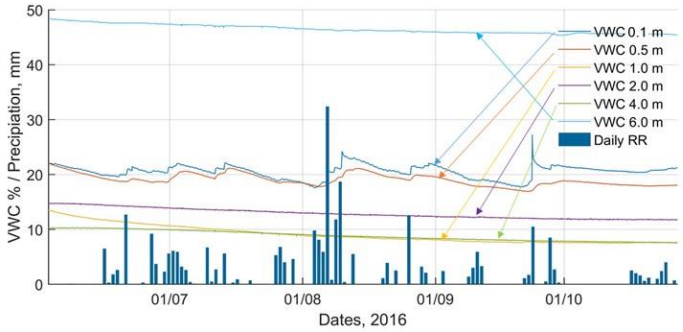

Figure 9. Volumetric water content from soil moisture sensors and daily rainfall (RR), June-October 2016.

A correlation analysis between change in water content and daily precipitation (gridded data) was performed (Fig. 10). For the shallowest sensor (at 0.1 m), $R^2 = 0.24$, which indicates some correlation. For deeper sensors, there was no statistical correlation between these variables. Although the statistical analysis shows poor correlation between rainfall and change in water content at large depth on the same day, correlations may be more successful for other pairs of variables. One alternative could be daily precipitation at "day X" correlated with change in water content at "day X+N", where N is a time shift to account for groundwater flow from the surface to the actual depth. N should then expectedly increase with depth. For presented data, such analyses seem rather useless, as there is almost no change in water content for deep sensors resulting from any observed scours. This may indicate that surface water flows towards the slope crest without infiltrating or that the damping/smoothening effect of the silt layer results in groundwater flow being spread over a considerable time so that individual scours are not present in the water content curves. Vertical water flow (flux) may also occur without water content increasing significantly.

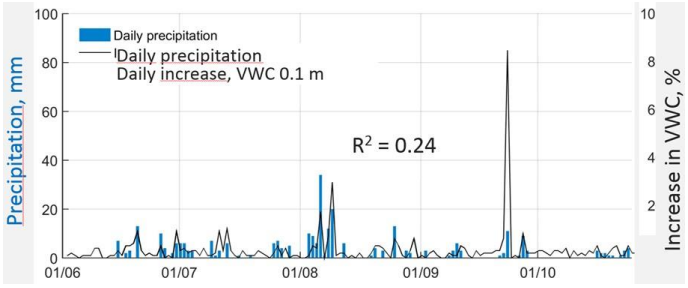

Figure 10. Correlation between water content in moisture sensors and daily precipitation (gridded data) June-October 2016.

Piezometers are very stable during the measurement period (Fig. 11). Changes are within ±a few kPa, verifying that hydrogeologic conditions for the sediment package do not allow for quick changes in the groundwater regime. The piezometers measure total pressure, including atmosphere.

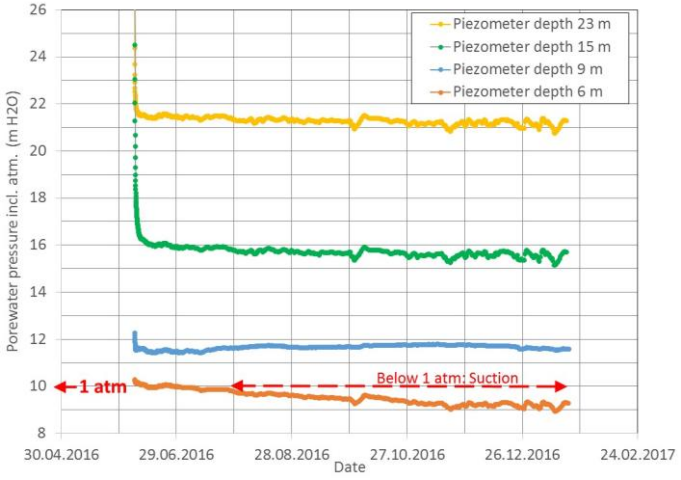

Figure 11. Piezometer readings in the period June 2016-January 2017. The piezometer at 6 m reads suction (lower pressure than atmospheric pressure).

An interesting observation is made from piezometer data at 6 m depth. In December 2016 pore-water pressure of 1 m below atmospheric pressure was measured, corresponding to groundwater level approx. 7 m. The piezometer at 9 m reads pore-water pressure corresponding to groundwater at 7 m (assuming hydrostatic pore-water pressure). These data support that, the observation at 6 m signifies soil suction of approx. 10 kPa.

6 RAINFALL AND SLOPE STABILITY

Using historical rainfall data from the region as input, seepage and slope stability analyses were performed. Analyses were done with the software package GeoStudio (GeoSlope International 2017); subpackage Seep/w for transient infiltration analysis and Slope/w for slope stability analysis.

6.1 *Rainfall*

Rainfall is a statistical variable, based on historical weather data, now also taking expected future climatic change into consideration. During the autumn of year 2000, a large number of landslides were triggered by extreme long-term rainfall in Eastern Norway. The number of landslides was particularly high in the area where the instrumented slope is located, i.e., the Romerike region north of Oslo. The year 2000 rainfall was found to have return period of > 100 years (Jaedicke & Kleven 2007). Daily rainfall records from year 2000 are shown in Figure 12. The rainfall record was used to model infiltration into the slope and to study the evolution of slope stability through the autumn of year 2000.

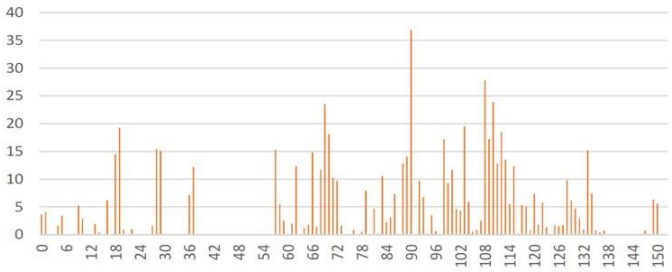

Figure 12. Daily rainfall 01 August – 31 December 2000.

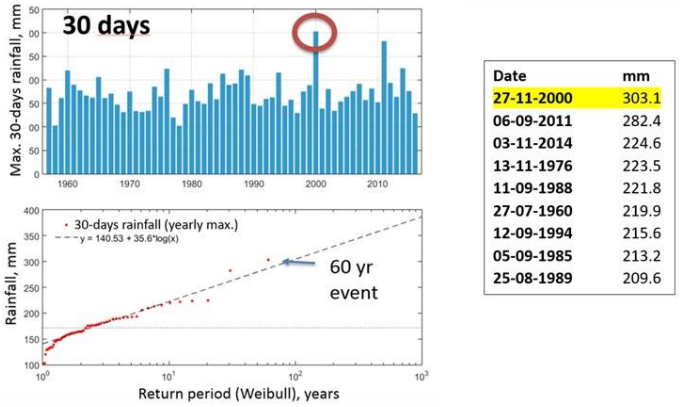

Date	mm
27-11-2000	303.1
06-09-2011	282.4
03-11-2014	224.6
13-11-1976	223.5
11-09-1988	221.8
27-07-1960	219.9
12-09-1994	215.6
05-09-1985	213.2
25-08-1989	209.6

Figure 13. Frequency analysis for 30 days duration of rainfall for the 60-year period 1957-2016.

A frequency analysis of rainfall records from nearby stations was performed for various rainfall durations (Fig. 13). For 30 days duration of rainfall, year 2000 has the highest measured rainfall, which for the analysed data gives a return period of 60 years. However, for a curve fit along the almost linear part of the curve (lin-log plot), the return period of the year 2000 rainfall is approx. 100 years. According to the table in Figure 13, the three highest 30-day periods have all occurred in year 2000 or later.

6.2 *Slope stability*

The stability of the steep upper slope was analysed, applying a drained Mohr-Coulomb model. Unsaturated soil strength was included as the product of suction and water content resulting from transient infiltration analyses, multiplied with the effective friction angle, i.e., Bishop stress with effective stress parameter χ=1 (Bishop 1960). The model has three layers: Sandy silt, clayey silt and clay (Fig. 14). Input parameters used in the analysis are given in Table 1. During infiltration, soil weight is corrected according to the retention curve.

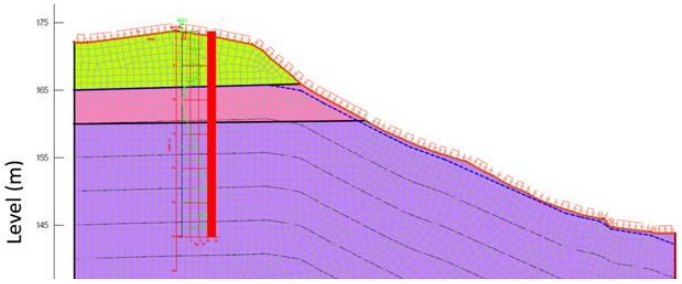

Figure 14. Model slope with three layers, from the top: Sandy silt, clayey silt and clay. Rotary pressure sounding shown.

Table 1. Summary of input soil strength parameters for slope stability analysis (total soil weight γ_{tot} given for saturated soil).

Layer	Soil type	ϕ (°)	c' (kPa)	γ_{tot} (kN/m^3)
1	Sandy silt	36	8	18
2	Clayey silt	32	8	18
3	Clay	26	5	19

Saturated permeability of the three layers in the calculations were set to 5E-06 m/s, 5E-07 m/s and 5E-09 m/s, respectively (higher in the top layer than actually measured to ensure that infiltration is not lower in the model than in situ). Permeability functions are shown in Figure 15. The clay layer is saturated throughout the analysis, while water content in the two other layers will change constantly with rainfall events and intermediate drought periods.

Seepage analysis was performed for a period of 135 days, taken from observed rainfall in year 2000 (Fig. 16a). The first 40 days of this period was "normal" (120-130 mm in 40 days), while the remaining period had very high rainfall. Slope stability was calculated after 40 days (09 September 2000), and resulted in a quite low slope safety factor for the "normal" rainfall situation, γ_m=1.09 (Fig. 16b). The groundwater line lies high in the clayey silt layer, with concentrated outflow of water at the boundary between clayey silt and clay (Fig. 16a).

For rainfall during the autumn of year 2000, stability analyses were performed for days 73 (12 October), 115 (24 November) and 134 (14 December). Day numbers refer to Figure 12. Slope safety factor for the failure surface in Figure 16 drops from 1.09 to γ_m=1.05, γ_m=0.96 and ends up at γ_m=0.97. Reduction in slope safety factor is approx. 10%. Based on the model, slope safety is critical at the end of the rainfall. The fact that the slope did not fail in year 2000, indicates that shear strength parameters are better than assumed. The natural slope probably has low safety; on the other hand, modelled change in

safety factor is quite small even during year 2000 rainfall.

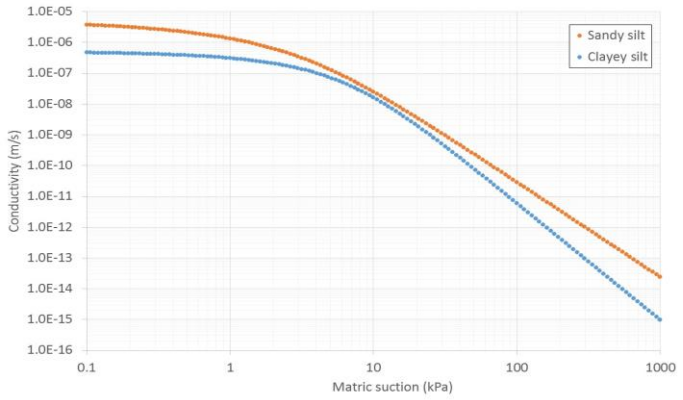

Figure 15. Permeability functions for sandy silt and clayey silt.

a)

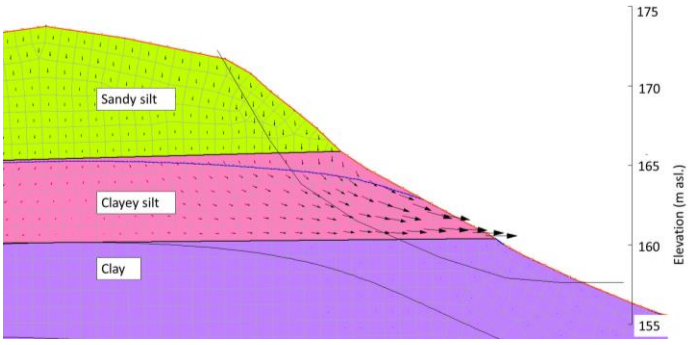

b)

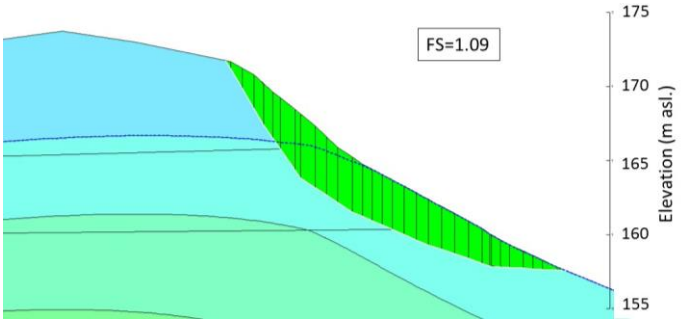

Figure 16. "Normal" rainfall conditions a) Seepage analysis with flow vectors b) Results from slope stability analysis

7 CONCLUSIONS

Instrumentation of a steep natural slope with soil moisture/temperature sensors and piezometers show that below 1 m, rainfall barely is reflected in changes in soil moisture. Seepage analysis was done based on extreme rainfall records from the autumn of year 2000. Calculated slope safety factor drops from 1.09 to 0.96 during rainfall. The slope remained stable in year 2000, which serves as an acid test of in situ conditions. Year 2000 rainfall had at least 100 years return period, implying a lower probability of slope failure than 0.01 per year. Whether this is satisfactory for nearby infrastructure needs to be clarified. Protective measures could be constructed to prevent landslide release or protect downslope infrastructure from impact from landslides. Application of unsaturated geomechanics in the slope study, combined with in situ instrumentation, improved the understanding of the situation and provides good background for calibration of the hydrogeological model. In future studies, longer time series will be available, and more work may be put into calibration of the hydrogeological model based on measured data.

8 ACKNOWLEDGEMENTS

The Norwegian national railway company, Bane NOR, and the client's representative, Terje Grønvold are acknowledged for allowing publishing of results from the project. Summer substitute at NGI in 2016, stud.tech. Johannes G. Holten is acknowledged for assisting in pressure plate testing.

9 REFERENCES

Bishop, A.W. 1959. The principle of effective stress. *Teknisk Ukeblad* 39: 859-863.

GeoSlope International. 2017. Geostudio, Seep/w and Slope/w.

Heyerdahl, H. & Pabst, T. 2017. Comparison of experimental and predictive approaches for determination of water retention curves of intact samples of Quaternary soils. G*eotechnical and geological engineering*: 1-21.

Heyerdahl, H. 2017. Influence of extreme long-term rainfall and unsaturated soil properties on triggering of a landslide – a case study. *Natural Hazards Earth System Science*. Discuss. https://doi.org/10.5194/nhess-2017-410, in review.

Hilf, J.W. 1956. An investigation of pore-water pressure in compacted cohesive soils. *Technical Memo, No. 654, U.S. Bureau of reclamation.*

Jaedicke, C. & Kleven, A. 2007. Long-term precipitation and slide activity in south-eastern Norway, autumn 2000. *Hydrological Processes* 22: 495-505.

van Genuchten, M.T. 1980. A closed-form equation for predicting the hydraulic conductivity of unsaturated soils. *Soil Sci. Soc. Am. J.* 44: 892-898.

Vanapalli, S.K., Fredlund, D.G., Pufahl, D.E. & Clifton, A.W. 1996. Model for the prediction of shear strength with respect to soil suction. *Canadian Geotechnical Journal* 33: 379-392.